Chemical Engineering Journal 151 (2009) 367–371

Contents lists available at ScienceDirect

Chemical Engineering Journal

journal homepage: www.elsevier.com/locate/cej

Studying the influence of process parameters on the catalytic carbon nanofibers formation using factorial design

Nabeel A. Jarrah*

Department of Chemical Engineering, Mutah University, P.O. Box 7, 61710 Karak, Jordan

ARTICLE INFO

Article history:
Received 16 December 2008
Received in revised form 8 March 2009
Accepted 26 March 2009

Keywords:
Carbon nanofibers
Nickel
Factorial design
Growth parameters

ABSTRACT

Carbon nanofibers were catalytically grown by the decomposition of C_2H_2/H_2 over an unsupported Ni catalyst. The aim of this article is to study the main and interaction effects of temperature (500–600 °C), H_2 flow rate (0–100 ml/min), and C_2H_2 flow rate (100–200 ml/min) on the yield and properties of carbon nanofibers. Full 2^3 factorial designs with three replicates at the center point and thus a total of 11 experiments were carried out. It turns out that when temperature increases there was a significant increase in the yield, in the BET, and also in the pore volume of the carbon nanofibers. On the other hand, increasing H_2 flow rate decreases the yield, the BET, and also decreases the pore volume of carbon nanofibers. Increasing C_2H_2 flow rate has an insignificant effect on the yield and it decreases the BET surface area and pore volume. The work shows that not only the effects of the main parameters are important, but also the interaction effects between them are significant. The study helps optimizing the process of carbon nanofibers growth.

© 2009 Elsevier B.V. All rights reserved.

1. Introduction

The formation of coke on metal catalyst *via* decomposition of carbon-containing gas has been known for long time [1]. It has been reported that the coke formation deactivates the active metal, deteriorate the pellets of the catalyst, and may damage the metallic reactor wall. Therefore, a great effort has been paid to limit the formation of coke [2–6].

On the other hand, researchers realized that the coke was mainly graphitic carbon nanofibers (CNF). The potential of CNF, as materials suitable for various applications, was reviewed by Rodriguez [7]. CNF have unique features, such as resistance to acidic/basic media, high mechanical strength, and high surface area without the presence of micropores [8–11]. These properties make CNF attractive to be utilized as catalyst support, adsorption agent, hydrogen storage, electrodes, composite materials, and polymer additives [7,12].

CNF can be catalytically produced by dissociating carbon-containing gas (e.g. CH_4, C_2H_4, C_2H_2, CO, etc.) on a surface of a metal catalyst (Ni, Fe, and Co) [13]. Many parameters may influence the yield and properties of the synthesized CNF, such as type of active metal, temperature, type of carbon-containing gas, gas velocity, gas partial pressure, run duration, hydrogen concentration, etc. Extensive studies were carried out both theoretically [14] and experimentally [15–21] in order to understand the influence of most of these parameters on CNF growth process. However, the most dominating process parameters in CNF growth are the flow rate of carbon-containing gas, the flow rate of hydrogen, and the growth temperature [22]. The effect of these parameters on the yield and morphology of CNF was studied by Yu et al. [22].

Conventional methods for studying the effect of some parameters on a process are done by varying one parameter by time maintaining all the other parameters constant. Then, the best value achieved by this procedure is fixed and other parameters are varied by time. The disadvantage of this univariate procedure is that the best conditions could not be attained, because the interaction effects between the parameters are discarded. Moreover, conventional methods are time consuming and require large number of experiments to determine the optimum conditions of a process. These drawbacks of the conventional methods can be eliminated by studying the effect of all parameters using factorial design [23,24]. It allows measuring the main effects of each parameter and interaction effect between parameters. To the best of our knowledge this is the first attempt to study the influence of growth parameters on the CNF process by applying factorial design. Most of previous studies [14–21] explored the effect of main parameters, but these studies did not clarify the interaction effects between parameters.

The aim of the present research is to carry out a factorial design study to determine the main and interaction effects of several parameters on the yield and properties of the CNF. Therefore, the effect of three parameters: temperature, H_2 flow rate, and C_2H_2 flow rate was studied. Further, empirical models correlating the

* Tel.: +962 3 2372380; fax: +962 3 2375540.
E-mail address: aljarrahn@mutah.edu.jo.

1385-8947/$ – see front matter © 2009 Elsevier B.V. All rights reserved.
doi:10.1016/j.cej.2009.03.057

Table 1
Experimental range and levels of independent process variables for CNF formation.

Independent parameters	Range (coded levels)		
	Low (−1)	Central point (0)	High (+1)
Temperature (X_1), °C	500	550	600
H_2 flow rate (X_2), ml/min	0	50	100
C_2H_2 flow rate (X_3), ml/min	100	150	200

yield, BET surface area, and pore volume of the CNF to the three parameters were developed.

2. Experimental

2.1. Catalyst preparation and CNF formation

2.1.1. Catalyst preparation

Nickel was prepared by precipitation of nickel carbonate from nickel nitrate solution, using ammonium bicarbonate (Aldrich 99%) at room temperature and pH of 9 ± 0.2 as described in detail elsewhere [13]. Nickel nitrate hexahydrate (12.5 g, Aldrich 99%) was dissolved in 500 ml of distilled water. Then, solid ammonium bicarbonate was added under stirring until the supernatant was colorless. The precipitate was filtered, dried at 100 °C, and calcined in static air at 500 °C for 2 h, in order to obtain nickel oxide.

2.1.2. Formation and characterization of CNF

The catalyst (100 mg), in its oxide form, was loaded in a stainless steel reactor with a porous ceramic plate at the bottom. The reactor was placed in a vertical electrical furnace (Carbolite, VST 12/300). The oxide was reduced at 500 °C (10 °C/min) for 2 h in a flow of 50% H_2 in N_2 (total flow rate = 200 ml/min). After reduction, the reactor was brought at the desired growth temperature, maintaining the 50% H_2 in N_2 flow. After reaching the desired temperature, the H_2 in N_2 flow was replaced by a mixture of C_2H_2 (100–200 ml/min) and H_2 (0–100 ml/min). The growth was carried out for 1.5 h. Then, the sample was cooled down to room temperature under N_2 stream. The amount formed of CNF was determined by weight and the yield of CNF was calculated by dividing the mass of CNF by the mass of Ni catalyst.

The primary structure of the CNF (BET surface area and pore volume) was studied by N_2 adsorption–desorption at 77 K.

2.2. Factorial design of experiment

Factorial design allows the simultaneous study of the effects that several parameters may have on an optimization of a particular process. A simple type of factorial design is that having two levels (low and high) for each parameter [23,24]. In a full-factorial design, responses are measured at all combinations of the experimental parameter levels. Factorial design allows measuring not only the main effect of each parameter, but also the interaction effect among all the parameters. The determination of interaction effects of parameters may be important for successful system optimization [23].

Growth temperature (X_1), H_2 flow rate (X_2), and C_2H_2 flow rate (X_3) were chosen as independent parameters and the responses studied were the yield of CNF (Y_1), BET surface area (Y_2), and pore volume (Y_3). Independent parameters, experimental range and coded levels for CNF formation are given in Table 1. A 2^3 full-factorial design, with three replicates at the center point and thus a total of 11 experiments were employed in this study. The center point replicates were chosen to evaluate the standard deviation of each parameter and to detect if there is any inflection point [23,24].

The results of the factorial design were studied and interpreted by MINITAB 14 software to estimate the response of the dependent parameter. Each response was modeled to the three studied parameters using the following equation:

$$Y_i = b_0 + b_1X_1 + b_2X_2 + b_3X_3 + b_{12}X_1X_2 + b_{13}X_1X_3 + b_{23}X_2X_3 + b_{123}X_1X_2X_3$$

where Y_i is the theoretical response function.

3. Results and discussion

The most important parameters, which affect the yield and properties of carbon nanofibers, are temperature, H_2 flow rate, and carbon-containing gas (i.e. C_2H_2) flow rate. The combined effects of these parameters were studied using factorial design of experiments. The ranges of the studied parameters are given in Table 1.

Table 2 presents the experimental responses (yield of CNF, BET surface area and pore volume) that have been measured at two levels of the studied parameters.

3.1. Statistical analysis

Polynomial regression models were developed using factorial design to analyze the effect of each parameter and the effect of its interactions with the other parameters on each response. Main effects, interaction effects, coefficients of the model, standard deviation of each coefficient, and probability for the 2^3 factorial design are presented in Table 3.

The *P*-value represents the probability of error that is involved in accepting our observed results [23]. Thus, the smaller the value of *P*, the more significant is the corresponding coefficient term. The final models in terms of coded parameters after excluding the insignificant terms (i.e. $P > 0.05$) for the yield (Y_1), BET surface area (Y_2), and pore volume (Y_3) of CNF are given in Eqs. (1)–(3), respectively.

$$Y_1 = 10.305X_1 - 6.312X_2 - 5.024X_1X_2 + 15.157 \quad (1)$$

$$Y_2 = 43.88X_1 - 11.13X_2 - 38.87X_3 + -7.13X_1X_2 - 44.88X_1X_3 + 7.12X_2X_3 \; 8.63X_1X_2X_3 + 117.38 \quad (2)$$

$$Y_3 = 8.125 \times 10^{-2}X_1 - 2.375 \times 10^{-2}X_2 - 6.875 \times 10^{-2}X_3 - 1.375 \times 10^{-2}X_1X_2 - 7.875 \times 10^{-2}X_1X_3 + 2.125 \times 10^{-2}X_2X_3 + 2.625 \times 10^{-7}X_1X_2X_3 + 0.20625 \quad (3)$$

Figs. 1–3 show the predicted values versus the experimental values of the yield, BET surface area, and pore volume, respectively. Fig. 1 shows some experimental data points that are not in full agreement with the model results. However, most of the predicted

Table 2
Full-factorial design matrix for CNF formation. Experimental responses of yield (Y_1), BET surface area (Y_2), and pore volume (Y_3) versus different levels of temperature (X_1), H_2 flow rate (X_2) and C_2H_2 flow rate (X_3).

Run	X_1	X_2	X_3	Yield (Y_1)	BET (Y_2)	Pore volume (Y_3)
1	−1	−1	−1	5.53	70	0.12
2	+1	−1	−1	40.25	279	0.52
3	−1	+1	−1	3.56	65	0.11
4	+1	+1	−1	10.18	211	0.35
5	−1	−1	+1	6.74	85	0.15
6	+1	−1	+1	33.34	80	0.13
7	−1	+1	+1	3.56	74	0.12
8	+1	+1	+1	18.07	75	0.15
9	0	0	0	20.47	153	0.23
10	0	0	0	26.09	144	0.22
11	0	0	0	24.18	147	0.22

Table 3
Full 2^3 factorial design for yield, BET, and pore volume versus temperature (X_1), H_2 flow rate (X_2), and C_2H_2 flow rate (X_3). Coefficients are given in coded units.

Term	Effect	Coefficient	S.E.[a]	P
(a) For yield (Y_1)				
Constant		15.157	1.01	0.004
X_1	20.609	10.305	1.01	0.009
X_2	−12.624	−6.312	1.01	0.025
X_3	0.547	0.273	1.01	0.812
$X_1 \times X_2$	−10.047	−5.024	1.01	0.038
$X_1 \times X_3$	−0.058	−0.029	1.01	0.98
$X_2 \times X_3$	3.398	1.699	1.01	0.235
$X_1 \times X_2 \times X_3$	4.002	2.001	1.01	0.186
(b) For BET surface area (Y_2)				
Constant		117.38	1.62	0.00
X_1	87.75	43.88	1.62	0.001
X_2	−22.25	−11.13	1.62	0.021
X_3	−77.75	−38.87	1.62	0.002
$X_1 \times X_2$	−14.25	−7.13	1.62	0.048
$X_1 \times X_3$	−89.75	−44.88	1.62	0.001
$X_2 \times X_3$	14.25	7.12	1.62	0.048
$X_1 \times X_2 \times X_3$	17.25	8.63	1.62	0.034
(c) For pore volume (Y_3)				
Constant		0.20626	2.041×10^{-3}	0.000
X_1	0.1625	0.08125	2.041×10^{-3}	0.001
X_2	−0.0475	−0.02375	2.041×10^{-3}	0.007
X_3	−0.1375	−0.06875	2.041×10^{-3}	0.001
$X_1 \times X_2$	−0.0275	−0.01375	2.041×10^{-3}	0.021
$X_1 \times X_3$	−0.1575	−0.07875	2.041×10^{-3}	0.001
$X_2 \times X_3$	0.0425	0.02125	2.041×10^{-3}	0.009
$X_1 \times X_2 \times X_3$	0.0525	0.02625	2.041×10^{-3}	0.006

[a] The standard error of a coefficient is the standard deviation of the difference between the estimated value of the coefficient and the true value.

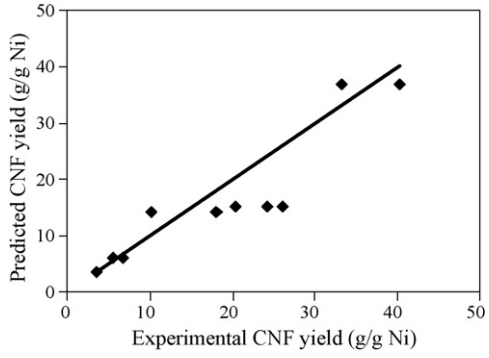

Fig. 1. Predicted versus experimental yield of carbon nanofibers from C_2H_2 decomposition on unsupported Ni.

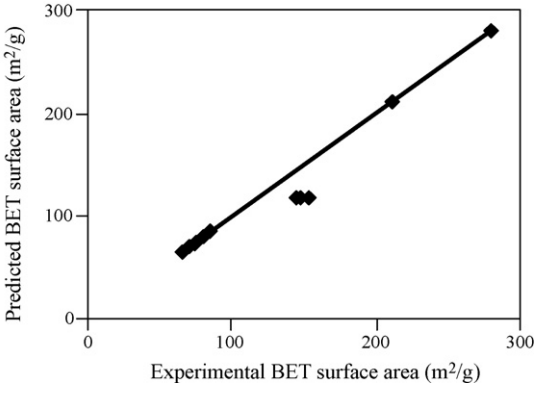

Fig. 2. Predicted versus experimental BET surface area of carbon nanofibers from C_2H_2 decomposition on unsupported Ni.

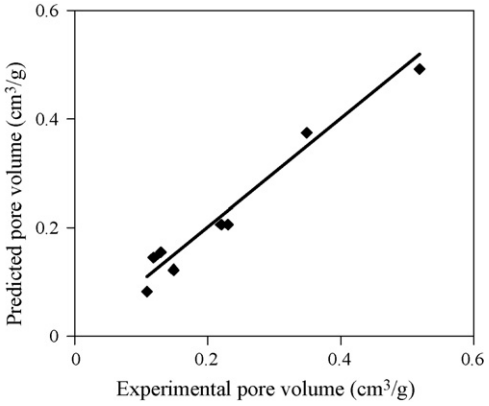

Fig. 3. Predicted versus experimental pore volume of carbon nanofibers from C_2H_2 decomposition on unsupported Ni.

values obtained (Figs. 1–3) were quite close to the experimental values, indicating that the models were successful in correlating the responses to the studied parameters.

It is clear that H_2 flow rate, temperature, and their interaction were significant at probability level ($P < 0.05$) for the yield of CNF. On the other hand, the C_2H_2 flow rate and all its interactions with the other parameters were insignificant (Table 3). For the BET surface area and pore volume, all the parameters and their interactions were significant at probability level ($P < 0.05$). The significance of these interaction effects between the parameters would have been lost if experiments were not carried out by factorial design.

3.2. Effect of parameters on CNF growth process

3.2.1. Yield of CNF

Fig. 4 shows the contour plot that relates the relative effects of temperature and H_2 flow rate on the yield of CNF when C_2H_2 flow rate is kept constant. It is clear that yield of CNF increases when temperature increases from 500 to 600 °C and when H_2 flow rate decreases from 100 ml/min to zero. Similarly, the yield of CNF was found to increase with temperature during the decomposition of $CO/C_2H_4/H_2$ over Fe–Cu and Ni–Fe catalysts [22] and also during the growth of carbon nanotubes from C_2H_2 decomposition on Ni, Fe and Co [25,26]. Romero et al. [21] found that when the ratio of H_2/C_2H_4 increases, the yield of the CNF decreases. Moreover, Pham-Huu et al. [25] showed that too large increase in hydrogen content during the decomposition of ethane on supported Ni catalyst resulted in a decrease in the yield of the CNF. On the other hand, different relationship between yield and H_2 flow rate has been reported from other studies [20,22]. Unexpectedly, C_2H_2 flow rate was found insignificant on the yield of CNF.

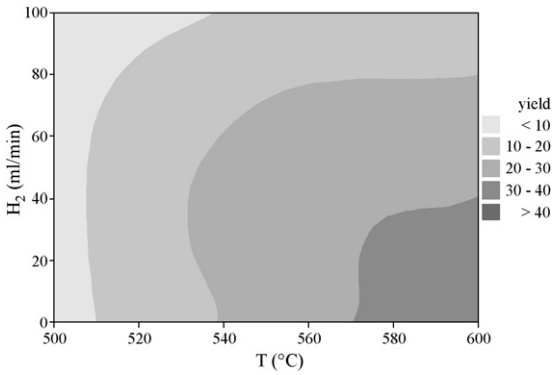

Fig. 4. Contour plot for the yield of carbon nanofibers (CNF) using C_2H_2.

Reviewing the mechanism of CNF formation is important to explain the influence of the studied parameters on the yield and properties of CNF. The mechanism has generally been accepted to include three steps: decomposition of the hydrocarbon on the surface of the Ni particles to form surface carbon; diffusion of the surface carbon through Ni; precipitation of the diffused carbon on the rare side of the Ni particle [8,10,27]. The process at the steady state is eventually a balance among the three steps, which means that when the steps are disturbed, the CNF growth will stop [10,13].

It is known that both hydrocarbon decomposition-rate and diffusion rate of carbon through nickel particles increase when temperature increases [28]. Thus, the yield of CNF is expected to increase with temperature. However, at very high temperature, hydrocarbon decomposition-rate, and hence carbon supply rate, exceeds carbon diffusion rate. As a result, carbon accumulates on the metal surface and partly deactivates the catalyst, leading to a decrease in the carbon yield [29]. Previous studies show a maximum yield within the studied temperature range [17,20,22,26,28]. Obviously, this range depends on the nature of the catalyst and the feedstock. Park and Keane [28] reported that the temperature-related carbon yield maximum is strongly dependent on the support material. Carneiro et al. [20] studied the growth of CNF from the decomposition of $CO/C_2H_4/H_2$ mixtures on Fe–Cu at temperature range of 500–650 °C. Optimum performance with respect to yield of CNF was found at 600 °C. Khedr et al. [29] produced CNF *via* decomposition of C_2H_2 on Fe at temperature range of 400–700 °C. They found that yield of carbon was maximum at 600 °C. Moreover, Solovyev et al. [30] studied the effect of temperature (400–700 °C) on the yield of CNF produced from propane decomposition on Ni and Ni–Cu catalysts. They found that 600 °C was the optimum temperature at which the yield of carbon was maximum. Similarly, our results show (Fig. 4) that the highest yield was achieved at 600 °C within the studied temperature range. However, our results show that yield increases with temperature, but no clear evidence shows that we are approaching a temperature-related carbon yield maximum within the studied temperature range.

Surprisingly, the model shows that the flow rate of C_2H_2 has an insignificant effect in the yield of CNF, despite the fact that more carbon species should be obtained at high flow rate of C_2H_2. This indicates that the increase in diffusion rate is the main reason behind increasing the yield of CNF at high temperature. It is generally believed that the intrinsic rate of CNF formation is controlled by diffusion rate of carbon through the Ni particle.

However, the effect of hydrogen on the formation of CNF is not straightforward [10]. The increase in the partial pressure of H_2 will decrease the formation rate of surface carbon due to two reasons: first, adsorped H_2 on the surface increases and that will suppress the dissociation of C_2H_2; second, H_2 will also enhance the gasification of the surface carbon. As a result, surface coverage of carbon decreases and that may decrease the yield of CNF [10].

3.2.2. BET surface area and pore volume of the CNF

The three parameters (temperature, H_2 flow rate, and C_2H_2 flow rate) and their interactions have significant effect on the BET surface area and pore volume of CNF. However, temperature (X_1), C_2H_2 flow rate (X_3), and their interaction were found to have the most significant effect, as indicated by very low P values. The contour plots given in Figs. 5 and 6 show the relative effects of temperature and C_2H_2 flow rate on BET surface area and pore volume, respectively. Figs. 5 and 6 show that both BET surface area and pore volume increase when temperature increases and C_2H_2 flow rate decreases. For example, the CNF with high BET surface area (279 m^2/g) exhibited a high pore volume (0.52 cm^3/g). On the other hand, the CNF with low surface area (65 m^2/g) exhibited a low pore volume (0.11 cm^3/g). Similarly, Toebes et al. [13] found that high surface area CNF (214 m^2/g) had high pore volume (0.41 cm^3/g) and low surface area CNF (54 m^2/g) had low pore volume (0.1 cm^3/g).

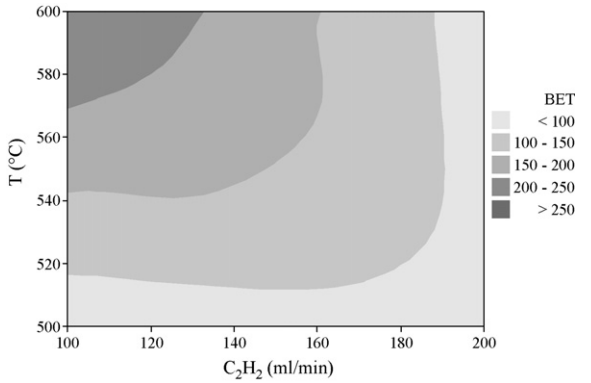

Fig. 5. Contour plot for the BET surface area of carbon nanofibers (CNF) using C_2H_2.

Generally, it is accepted that the diameter of CNF increases (i.e. BET surface area decreases) when growth temperature increases. This is attributed to two main reasons: first, the mobility of Ni increases at high temperature, leading to the formation of larger metal clusters that grow thicker CNF, which is in agreement that the diameter of CNF is controlled by the size of Ni particles [8]; second, uncatalyzed thermal decomposition of the carbon-containing gas is leading to pyrolytic over-coating of the underlying CNF [15,17,22,31].

At the contrary, Fig. 5 shows that BET surface area increases when temperature increases at low flow rate of C_2H_2. This means that, small Ni particles have a higher contribution for the growth of CNF than the larger ones. This different behavior is justified by two reasons: First, metal particles fragmentized during the growth of CNF. Tanaka et al. [32] found that diameter of CNF decreases, and hence BET surface area increases when temperature increases from 580 to 630 °C. They concluded that large Fe–Ni clusters fragmentized into small particles at high temperature. Similarly, Park and Keane [28,31] showed that thin CNF were formed using ethylene decomposition on large Ni particles. The authors also concluded that fragmentation took place during growth. Second, it is known that small Ni particles grow CNF faster than larger ones and have a higher contribution to the ultimate carbon growth [31]. Moreover, large particles might be not active at all for CNF growth [16].

Our results (Figs. 4–6) show that there are significant interaction effects between the studied parameters on the yield, BET surface area, and pore volume of the CNF. Factorial design of experiments allowed us to study and understand not only the main effect of each parameter on the process of CNF growth, but also the effect from the interaction between parameters.

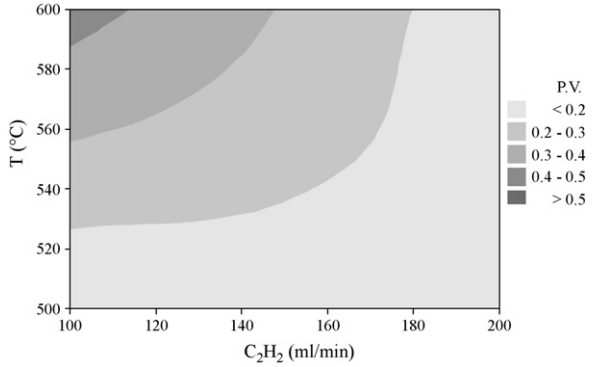

Fig. 6. Contour plot for the pore volume (P.V.) of carbon nanofibers (CNF) using C_2H_2.

4. Conclusions

In this work we study the growth of CNF from C_2H_2/H_2 mixture over unsupported Ni catalyst. The process has been studied with respect to temperature, H_2 flow rate, and C_2H_2 flow rate using factorial design of experiments.

It turns out that when temperature increases there was a significant increase in the yield, in the BET, and also in the pore volume of the carbon nanofibers. On the other hand, Increasing H_2 flow rate decreases the yield, the BET, and also decrease the pore volume of carbon nanofibers. Increasing C_2H_2 flow rate has an insignificant effect on the yield and it decreases the BET surface area and pore volume.

Satisfactory empirical models were developed to correlate the growth parameters to the yield and textural properties of CNF. This study helps to optimize the operating parameters in order to control the yield and properties of CNF.

Acknowledgments

The author acknowledges Sami Alkredmi for BET measurement and Ali Alzoubi for technical help (The financial support from Mutah University is gratefully acknowledged).

References

[1] R.T.K. Baker, Electron microscopy studies of the catalytic growth of carbon filaments, in: J.L. Figueiredo, C.A. Bernardo, R.T.K. Baker, K.J. Huttinger (Eds.), Carbon Fibers, Filaments and Composites, Kluwer Academic, 1990, pp. 405–439.
[2] Z. Li, J. Chen, X. Zhang, Y. Li, K.K. Fung, Catalytic synthesized carbon nanostructures from methane using nanocrystalline Ni, Carbon 40 (2002) 409–415.
[3] D.L. Trimm, The formation and removal of coke from nickel catalyst, Catal. Rev. Sci. Eng. 16 (2) (1997) 155–189.
[4] C.H. Bartholomew, Carbon deposition in steam reforming and methanation, Catal. Rev. Sci. Eng. 24 (1) (1982) 67112.
[5] J.R. Rostrup-Nielsen, Industrial relevance of coking, Catal. Today 37 (1997) 225–232.
[6] J. Sehested, Four challenges for nickel steam-reforming catalysts, Catal. Today 111 (2006) 103–110.
[7] N.M. Rodriguez, A review of catalytically grown carbon nanofibers, J. Mater. Res. 8 (12) (1993) 3233–3250.
[8] K.P. de Jong, J.W. Geus, Carbon nanofibers: catalyst synthesis and applications, Catal. Rev. Sci. Eng. 42 (4) (2000) 481–510.
[9] P. Serp, M. Corrias, P. Kalck, Carbon nanotubes and nanofibers in catalysis—review, Appl. Catal. A: Gen. 253 (2003) 337–358.
[10] D. Chen, K.O. Christensen, E. Ochoa-Fernandez, Z. Yu, B. TØtdal, N. Latorre, A. Monzon, A. Holmen, Synthesis of carbon nanofibers: effect of Ni crystal size during methane decomposition, J. Catal. 229 (2005) 82–96.
[11] N. Jarrah, F. Li, J.G. van Ommen, L. Lefferts, Immobilization of layer of carbon nano-fibers (CNFs) on Ni foam: a new structured catalyst support, J. Mater. Chem. 15 (2005) 1946–1953.
[12] Z. Yu, D. Chen, M. RØnning, B. TØtdal, T. Vralstad, E. Ochoa-Fernandez, A. Monzon, A. Holmen, Large-scale synthesis of carbon nanofibers on Ni–Fe–Al hydrotalcite derived catalysts. II. Effect of Ni/Fe composition on CNF synthesis from ethylene and carbon monoxide, Appl. Catal. A: Gen. 338 (2008) 147–158.
[13] M.L. Toebes, J.H. Bitter, A. van Dillen, K.P. de Jong, Impact of the structure and reactivity of nickel particles on the catalytic growth of carbon nanofibers, Catal. Today 76 (1) (2002) 33–42.
[14] M. Grujicic, G. Cao, B. Gersten, Optimization of the chemical vapor deposition process for carbon nanotubes fabrication, Appl. Surf. Sci. 199 (2002) 90–106.
[15] C. Singh, M. Shaffer, A. Windle, Production of controlled architectures of aligned carbon nanotubes by an injection chemical vapour deposition method, Carbon 41 (2003) 359–368.
[16] D. Venegoni, P. Serp, R. Feurer, Y. Kihn, C. Vahlas, P. Kalck, Parametric study for the growth of carbon nanotubes by catalytic chemical vapor deposition in a fluidized bed reactor, Carbon 40 (2002) 1799–1807.
[17] Ch. Veziri, G. Pilatos, G. Karanikolos, A. Labropoulos, K. Kordatos, V. Kasselouri-Rigopoulou, N. Kanellopoulos, Growth and optimization of carbon nanotubes in activated carbon by catalytic chemical vapor deposition, Micropor. Mesopor. Mater. 110 (2008) 41–50.
[18] M. Castro Díaz, J. Blackman, C. Snape, Maximising carbon nanofiber and hydrogen production in the catalytic decomposition of ethylene over an unsupported Ni–Cu alloy, Appl. Catal. A: Gen. 339 (2008) 196–208.
[19] M. Escobar, M. Moreno, R. Candal, M. Claudia Marchi, A. Caso, P. Polosecki, G. Rubiolo, S. Goyanes, Synthesis of carbon nanotubes by CVD: effect of acetylene pressure on nanotubes characteristics, Appl. Surf. Sci. 254 (2007) 251–256.
[20] O.C. Carneiro, N.M. Rodriguez, R.T.K. Baker, Growth of carbon nanofibers from the iron–copper catalyzed decomposition of $CO/C_2H_4/H_2$ mixtures, Carbon 43 (2005) 2389–2396.
[21] A. Romero, A. Garrido, A. Nieto-Márquez, A. Raquel de la Osa, A. de Lucas, J. Valverde, The influence of operating conditions on the growth of carbon nanofibers on carbon nanofiber-supported nickel catalysts, Appl. Catal. A: Gen. 319 (2007) 246–258.
[22] Z. Yu, D. Chen, B. TØtdal, A. Holmen, Parametric study of carbon nanofiber growth by catalytic ethylene decomposition on hydrotalcite derived catalysts, Mater. Chem. Phys. 92 (2005) 71–81.
[23] D.C. Montgomery, Design and Analysis of Experiments, 5th ed., John Wiley & Sons, New York, 2001.
[24] G.E.P. Box, W.G. Hunter, J.S. Hunter, Statistics for Experiments—An Introduction to Design, Data Analysis and Model Building, John Wiley & Sons, New York, 1978.
[25] C. Pham-Huu, N. Keller, V.V. Roddatis, G. Mestl, R. Schlogl, M.J. Ledoux, Large scale synthesis of carbon nanofibers by catalytic decomposition of ethane on nickel nanoclusters decorating carbon nanotubes, Phys. Chem. Chem. Phys. 4 (2002) 514–521.
[26] A. Kukovecz, Z. Konya, N. Nagaraju, I. Willens, A. Tamasi, A. Fonseca, J.B. Nagy, I. Kiricsi, Catalytic synthesis of carbon nanotubes over Co, Fe and Ni containing conventional and sol–gel silica–aluminas, Phys. Chem. Chem. Phys. 2 (2000) 3071–3076.
[27] R.T.K. Baker, P.S. Harris, R.B. Thomas, R.J. Waite, Formation of filamentous carbon from iron, cobalt and chromium catalyzed decomposition of acetylene, J. Catal. 30 (1973) 86–95.
[28] C. Park, M. Keane, Catalyst support effects in the growth of structured carbon from the decomposition of ethylene over nickel, J. Catal. 221 (2004) 386–399.
[29] M.H. Khedr, K.S. Abdel Halim, N.K. Soliman, Effect of temperature on the kinetic of acetylene decomposition over reduced iron oxide catalyst for the production of carbon nanotubes, Appl. Surf. Sci. 255 (2008) 2375–2381.
[30] E.A. Solovyev, D.G. Kuvshinov, DYu. Ermakov, G.G. Kuvshinov, Production of hydrogen and nanofibrous carbon by selective catalytic decomposition of propane, Int. J. Hydrogen Energy 34 (2009) 1310–1323.
[31] C. Park, M. Keane, Controlled growth of highly ordered carbon nanofibers from Y zeolite supported Ni catalyst, Langmuir 17 (2001) 8386–8396.
[32] A. Tanaka, S. Yoon, I. Mochida, Formation of fine Fe–Ni particles for the non-supported catalytic synthesis of uniform carbon nanofibers, Carbon 42 (2004) 1291–1298.